RESEARCH ARTICLE

The pathology of sponge orange band disease affecting the Caribbean barrel sponge *Xestospongia muta*

Hilde Angermeier[1], Janine Kamke[1], Usama R. Abdelmohsen[1], Georg Krohne[2], Joseph R. Pawlik[3], Niels L. Lindquist[4] & Ute Hentschel[1]

[1]Julius-von-Sachs-Institute for Biological Sciences, University of Wuerzburg, Wuerzburg, Germany; [2]Biocenter, Division of Electron Microscopy, University of Wuerzburg, Wuerzburg, Germany; [3]Department of Biology and Marine Biology, Center for Marine Science, University of North Carolina Wilmington, NC, USA; and [4]Institute of Marine Sciences, University of North Carolina at Chapel Hill, NC, USA

Correspondence: Ute Hentschel, Julius-von-Sachs-Institute for Biological Sciences, University of Wuerzburg, Wuerzburg D-97070, Germany. Tel.: +49 931 31 82581; fax: +49 931 31 86235; e-mail: ute.hentschel@uni-wuerzburg.de

Abstract

The aim of this study was to examine sponge orange band (SOB) disease affecting the prominent Caribbean sponge *Xestospongia muta*. Scanning and transmission electron microscopy revealed that SOB is accompanied by the massive destruction of the pinacoderm. Chlorophyll *a* content and the main secondary metabolites, tetrahydrofurans, characteristic of *X. muta*, were significantly lower in bleached than in healthy tissues. Denaturing gradient gel electrophoresis using cyanobacteria-specific 16S rRNA gene primers revealed a distinct shift from the *Synechococcus/Prochlorococcus* clade of sponge symbionts towards several clades of unspecific cyanobacteria, including lineages associated with coral disease (i.e. *Leptolyngbya* sp.). Underwater infection experiments were conducted by transplanting bleached cores into healthy individuals, but revealed no signs of SOB development. This study provided no evidence for the involvement of a specific microbial pathogen as an etiologic agent of disease; hence, the cause of SOB disease in *X. muta* remains unidentified.

Introduction

To date, coral diseases have received enormous attention owing to the important role of coral reefs in global biodiversity as well as the alarming rate at which reefs have been decimated in the context of global warming (Rosenberg *et al.*, 2007; Mao-Jones *et al.*, 2010). In comparison, much less effort has been undertaken to investigate diseases of marine sponges. Disease epidemics can in fact cause drastic reductions of sponge populations, with negative effects on the overall reef ecology (Webster, 2007). Sponge diseases have been documented in all major ocean bodies, with the Caribbean representing a particular hot spot (Harvell *et al.*, 1999). They typically start with the appearance of discolored patches, followed by tissue disintegration, leaving behind the exposed skeleton. The size and consistency of the sponge seem to affect the pattern of disease progression, which may spread over the entire body within weeks to months. It is noteworthy that the disease typically does not switch host species for reasons that are not understood. Research on sponge diseases is hampered by the fact that the death of any given sponge often goes unnoticed.

The factors that cause disease in sponges are still largely unknown. A clear correlation has been documented between high (Cerrano *et al.*, 2000; Perez *et al.*, 2000; Lopez-Legentil *et al.*, 2008; Webster *et al.*, 2008a; Maldonado *et al.*, 2010) and low temperatures (Perez *et al.*, 2006) and sponge disease. The role of temperature is important in the context of global warming and climate change, which impact the composition of entire ecosystems (Hughes *et al.*, 2003; Hoegh-Guldberg *et al.*, 2007; Whiteman, 2010). Among other abiotic factors, hurricanes, physical damage and water turbidity do not seem to be major causes of sponge death (Wulff, 2006). Exposure of the sponge *Rhopaloeides odorabile* to the heavy metal copper has been shown to cause severe necrosis as well as shifts in its microbial community composition (Webster *et al.*, 2001). Even though it has been difficult to pinpoint the exact causes, environmental stress is likely to decrease the fitness of sponges, which may, in turn, render them more susceptible to disease.

Diverse microorganisms such as *Alphaproteobacteria* (Webster *et al.*, 2002), representatives of the genera *Bacillus* and *Pseudomonas* (Cervino *et al.*, 2006), cyanobacteria (Rützler, 1988; Olson *et al.*, 2006), fungi (Galstoff, 1942) and viruses (Vacelet & Gallissian, 1978) have been implicated as disease-causing agents among sponges. However, in only one case have Koch's postulates been upheld, linking a causative microorganism to a specific disease (Webster *et al.*, 2002). A number of additional studies implicated microbial pathogens as etiological agents of sponge disease (Webster, 2007); however, a bona fide sponge pathogen has rarely been identified. Recently, there has been a paradigm shift in that environmental factors rather than infectious agents are considered as the main causes of sponge disease (Luter *et al.*, 2010).

Our study focuses on the barrel sponge *Xestospongia muta* (*Demospongiae*, *Haplosclerida*), one of the largest, oldest and most common members of Caribbean coral reef communities (Armstrong *et al.*, 2006; McMurray *et al.*, 2008) and a species whose populations are increasing as coral cover has decreased (McMurray *et al.*, 2010). Unsaturated polyacetylenic brominated acids (Ashok *et al.*, 1992), xestosterol and mutasterol have been isolated from *X. muta* (Li *et al.*, 1981). Recently, a family of chiral tetrahydrofurans, mutafurans A–G, with antifungal activities has been obtained from this sponge species (Morinaka *et al.*, 2007). *Xestospongia muta* harbors dense and phylogenetically distinct microbial communities extracellularly within its mesohyl and is therefore a representative of the high microbial abundance (HMA) group of sponges (Hentschel *et al.*, 2006). The surface layers (pinacoderm) are populated by the *Synechococcus*/*Prochlorococcus* clade of cyanobacterial symbionts, which are also responsible for the distinctive, reddish-brown surface coloration (Steindler *et al.*, 2005). Vertical transmission of its microbial symbionts through the reproductive elements has been demonstrated (Schmitt *et al.*, 2008).

Massive bleaching events of Caribbean *X. muta* specimens were observed in Puerto Rico (Vicente, 1990), Belize and the Florida Keys (Gammill & Fenner, 2005), Curaçao (Nagelkerken *et al.*, 2000) as well as offshore Cuba and the reefs of Cozumel (Mexico) (Gammill & Fenner, 2005). The most recent outbreak took place in June of 2009 in the US Virgin Islands, where approximately 20% of the resident *X. muta* population was affected (T. Smith, pers. commun.). Two types of bleaching have been described: cyclic bleaching, from which sponges recover, and fatal bleaching, synonymous with sponge orange band (SOB) disease, which usually results in sponge death (Cowart *et al.*, 2006; Lopez-Legentil *et al.*, 2008). The disease starts with lesions on the outer surface and spreads over the sponge body within weeks, leaving exposed skeleton behind. SOB is frequently accompanied by an orange transition band, giving rise to the name (Cowart *et al.*, 2006). In the present study, we aimed to provide an in-depth characterization of the pathology of fatal SOB disease as well as changes in the chemical and microbial community profiles during disease progression. Furthermore, attempts to prove Koch's postulates were undertaken by conducting underwater infection experiments.

Materials and methods

Sponge collection

Samples of healthy and diseased *X. muta* sponges (class *Demospongiae*, order *Haplosclerida*, family *Petrosiidae*) were collected by SCUBA at a depth of 4–30 m within the Florida Keys National Marine Sanctuary in November and December 2007 and September 2009. Additional sampling was conducted in June 2007 and 2008 during research expeditions throughout the Bahamas onboard the *RV Seward Johnson II*. The samples were transferred to the surface in seawater-containing Ziploc bags and kept cool until further processing within 1–2 h. Altogether, seven healthy and 12 diseased individuals were obtained. The term sponge 'tissue' is used hereafter in a colloquial sense, as sponges are made up of a confederation of cell types and do not have true tissues or organs (Brusca & Brusca, 1990).

Electron microscopy

Scanning electron microscopy (SEM) was performed on pieces of tissue of 0.5 cm^3 size from selected *X. muta* specimens following established protocols by Scheuermayer *et al.* (2006). Briefly, this involved the excision of sponge tissue, storage in 6.25% glutaraldehyde phosphate-buffered solution, washing procedures with Soerensen phosphate buffer (50 mM, pH 7.4) and dehydration in an increasing acetone series. The samples were critical point dried, sputtered with gold-palladium and stored in the dehydrator until examination using the scanning electron microscope (Zeiss DSM 962, Oberkochen, Germany). Transmission electron microscopy (TEM) was performed on pieces of tissue of about 1.0 mm^3 size from selected *X. muta* individuals following the procedure of Schmitt *et al.* (2008). The prepared samples were sectioned using an MT-7000 ultramicrotome (RMC, Tuscon, AZ) for examination with the transmission electron microscope (Zeiss EM10).

Chlorophyll *a* analysis

Chlorophyll *a* content was measured via spectrophotometry (Parsons *et al.*, 1984) on three 0.5 g tissue cubes per individual. The samples were maintained in a 90% acetone : water mixture at 4 °C in the dark until analysis. After centrifugation, the absorbance of 1 mL supernatant was measured at 750, 664, 647 and 630 nm using an optic spectrophotometer (Amersham Biosciences, Ultrospec 3100

pro). The chlorophyll *a* content was calculated using the equations of Parsons *et al.* (1984) and standardized to the volume of sponge tissue.

HPLC

Lyophilized sponge samples were ground with a mortar and pestle and extracted overnight by stirring at room temperature with twice the volume of 100% methanol. After vacuum filtration, the supernatants were dried on a rotary evaporator at $40\,°C$. For each extract, $5.0\,mg$ were dissolved in $1.0\,mL$ of methanol, from which $5.0\,\mu L$ was analyzed via analytical HPLC using a Jasco system (pump PU1580, gradient unit LG-980-025, degasser DG-2080-53 and UV detector MD-2010Plus) on a Chromolith RP-18e column ($4.6 \times 100\,mm$; Merck). The separation was achieved with a solvent mixture of acetonitrile and water complemented with 0.05% trifluoroacetic acid, starting with 10% acetonitrile : H_2O to 100% acetonitrile over a time span of 15 min and at a flow rate of $3\,mL\,min^{-1}$.

Preparative isolation was carried out using an HPLC Jasco system (pump PU1580, gradient unit LG-980-025, degasser DG-2080-53 and UV detector MD-2010Plus) on a Chromolith SemiPrep RP-18e column ($10 \times 100\,mm$; Merck). A solvent gradient of 10% acetonitrile : H_2O to 100% acetonitrile supplemented with 0.05% trifluoroacetic acid was used over a time span of 15 min at a flow rate of $10\,mL\,min^{-1}$. HPLC–ESI-MS/MS analysis was performed on $5.0\,\mu L$ of healthy *X. muta* extract utilizing a triple-stage quadrupole 7000 tandem mass spectrometer system equipped with an ESI interface (Finnigan MAT, Bremen, Germany). Data acquisition and evaluation were conducted on DEC 5000/33 digital equipment (Unterfoehring, Germany) using ICIS 8.1 software (Finnigan MAT). Positive ions were detected by scanning from 170 to 900 u with a 1-s scan duration for a single spectrum.

Denaturing gradient gel electrophoresis (DGGE)

For DNA extraction, sponge samples preserved in 70% ethanol and $0.5\,cm^3$ in size were air-dried and homogenized with a mortar and pestle in liquid nitrogen. The DNA extraction and 16S rRNA gene amplification for DGGE were performed as described in Schmitt *et al.* (2008), with the following modifications: the primer pair 106f with a GC-clamp and 781r was used for PCR amplification of the cyanobacterial 16S rRNA gene (Nübel *et al.*, 1997) and the primer pair 341f with a GC-clamp and 907r (Muyzer *et al.*, 1998) was used for the bacterial 16S rRNA gene. The PCR was conducted using a T3 Thermocycler (Biometra, Germany) using the following conditions: initial denaturation at $94\,°C$ for 2 min, 34 cycles of denaturation at $94\,°C$ for 1 min, primer annealing at $60\,°C$ (cyanobacterial primers) or $57\,°C$ (bacterial primers) for 1 min following elongation at $72\,°C$ for 75 s.

The final extension step was at $72\,°C$ for 10 min. The size and quality of the PCR products obtained were examined on 2% agarose gels following staining with ethidium bromide. DGGE was conducted as described by Schmitt *et al.* (2008) on 8% w/v polyacrylamide gels. Selected DGGE bands were excised under UV-light using an ethanol-sterilized scalpel and extracted overnight with $25\,\mu L$ H_2O at $4\,°C$. Cluster analyses of the DGGE banding pattern were conducted using the software program QUANTITY ONE (Bio-Rad, Munich, Germany). Dendrograms were constructed using the UPGAMA clustering method as defined by QUANTITY ONE to compare the banding pattern similarities in between different samples within one gel.

Cloning and sequencing

The excised DGGE bands were reamplified with the primers 106f and 781r (Nübel *et al.*, 1997), and the obtained PCR products were purified, ligated into the vector pGEM-T-Easy (Promega) and transformed into *Escherichia coli* Nova-Blue cells. The plasmid DNA was isolated using standard miniprep procedures (Sambrook *et al.*, 1989) and digested with EcoRI to confirm the correct insert size by agarose gel electrophoresis. Sequencing was conducted for up to four clones per DGGE band as described in Schmitt *et al.* (2008). Chimeras were identified using the program PINTAIL (Ashelford *et al.*, 2005) by comparison against the five most closely related 16S rRNA gene sequences from culturable bacteria and removed from the dataset.

Phylogenetic analysis

The ARB program package (Ludwig *et al.*, 2004) was used for sequence alignment and phylogenetic tree construction. The derived *X. muta* sequences and their closest basic local alignment search tool (BLAST) hits were imported into the SILVA 16S rRNA gene database (version 93) (Pruesse *et al.*, 2007) for automatic alignment and manual refinement using the ARB integrated alignment tool. Only sequences $\geq 1200\,bp$ were used for the calculation of neighbor joining, maximum likelihood and maximum parsimony trees. Shorter sequences were added using the parsimony interactive tool in ARB without changing the tree topology. All trees were constructed using conservation filters for cyanobacteria and bootstrap analysis (1000 resamplings). The resulting trees were compared and the maximum likelihood tree was chosen for publication. The highlighted group was supported by all three treeing methods. All 16S rRNA gene sequences were deposited in GenBank (accession numbers GU590802–GU590859).

Infection experiments

The experiments were conducted at a water depth of $\sim 20\,m$ on Conch Reef ($24°56'863''N$; $80°27'230''W$). For this

purpose, tissue samples of 1.5 cm diameter and ~5 cm depth were removed with a corkborer from diseased sponges and placed in healthy individuals where identical holes had been created. Nine tissue cores were removed per diseased sponge and three cores were placed into each of three healthy individuals. This experiment was performed for a total of three diseased sponges and, in the same fashion, for one healthy individual as a control, resulting in a total of 36 transplanted cores. The overall health condition of the transplanted sponges was monitored regularly by SCUBA over 11 days.

Results

Underwater photography

Healthy specimens of *X. muta* are barrel-shaped and have a brown, irregular surface, often with protrusions (Fig. 1a). Diseased individuals show a distinctive change from brown to a bleached white color. Bleaching typically starts as isolated patches penetrating the first few millimeters of the surface tissue (Supporting Information, Fig. S1). Eventually, the entire sponge body may be affected (Fig. 1b and c). This transition can be accompanied by an orange band, giving rise to the name 'sponge orange band' of this disease (Fig. 1b–d; Cowart *et al.*, 2006). However, an orange band was observed only in about half of the sponges investigated in this study. In addition to color loss, massive tissue destruc-

tion and erosion was observed (Fig. 1d), which usually leads to the collapse of the entire sponge. Only sponges in the early stage of disease were actively pumping, as judged visually by the application of fluorescent dye, while the water flow had ceased in sponges in the advanced stages of disease.

Electronmicroscopical observations

Tissues from five healthy and five diseased *X. muta* were inspected by SEM. Representative images of one healthy and one diseased individual (Fig. 1d) are shown. SEM on the surfaces of healthy *X. muta* revealed characteristic features. The ostia are visible as opening canals and the spicules are readily identified as spines embedded within the extracellular matrix (Fig. 2a). The flattened pinacocyte cells form an incoherent layer covering large areas of the mesohyl matrix (Fig. 2b). In contrast, the outer layers of the white tissues of a diseased sponge are made up of spicule material and only very little biomass is left (Fig. 2c). In the enlargement, filaments resembling bacteria are found to cover the spicules (Fig. 2d).

Particular care was taken to visualize the cellular processes in the orange band transition zone. For this purpose, samples were compared from sponges collected in the Bahamas (one healthy and two diseased individuals investigated), which appeared to be in an early stage of disease, and from Florida (two healthy and three diseased individuals
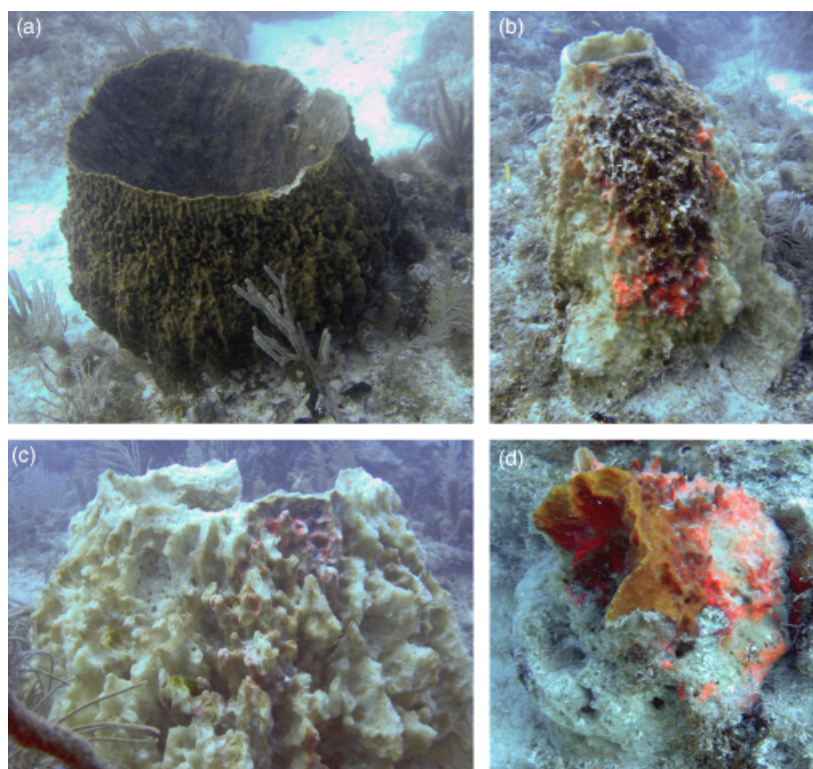

Fig. 1. Underwater photographs of representative *Xestospongia muta* individuals: healthy individual #9 (a) and individuals #4, #3 and #5 in advanced stages of disease (b, c, d). Underwater photography by Hilde Angermeier.
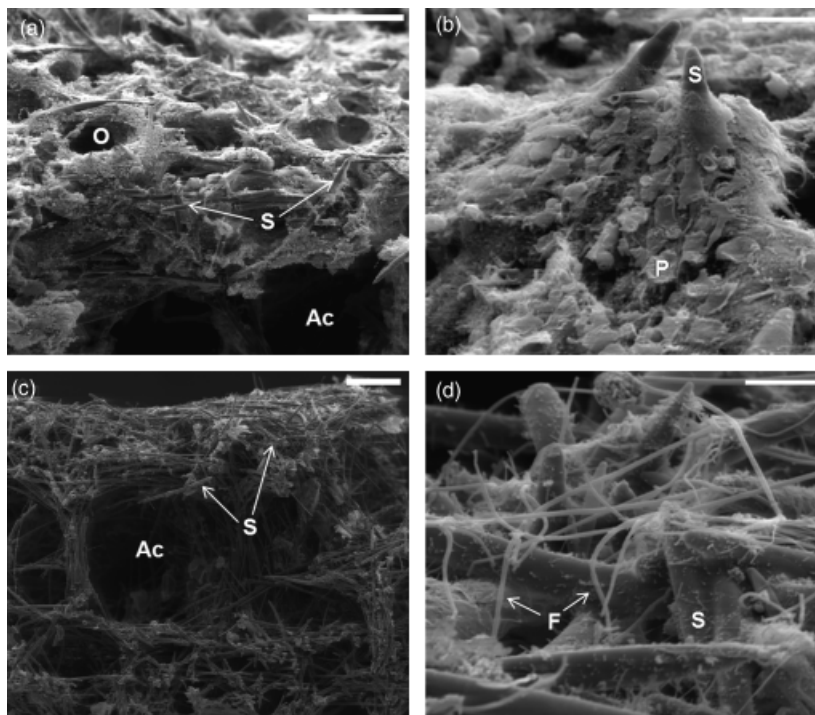
Fig. 2. Scanning electron micrographs of the surfaces of healthy (a, b) and diseased (c, d) *Xestospongia muta* individuals. The scale bars represent 200 μm (a, c) and 20 μm (b, d). O, osculi; S, spicules; P, pinacocytes; Ac, aquiferous canals; F, filaments.
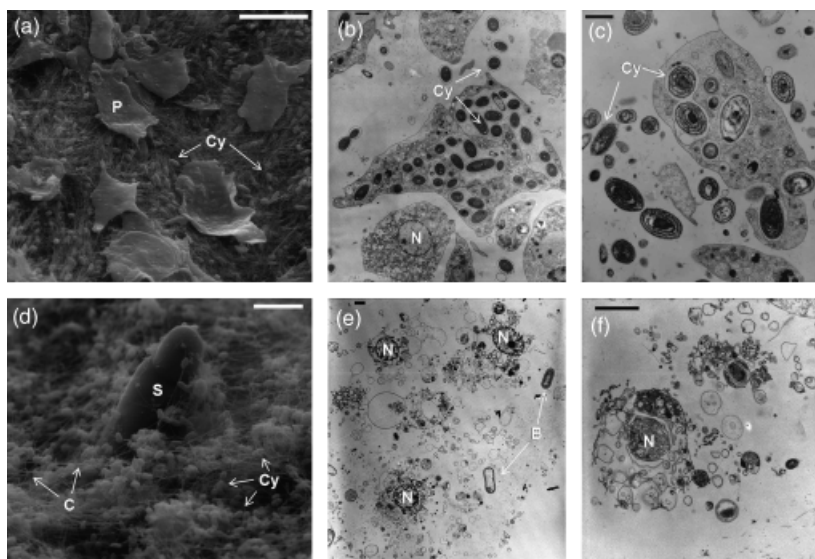

Fig. 3. Scanning electron micrographs of the orange band transition zone of *Xestospongia muta* sponges collected from the Bahamas (a–c) and from Florida (d–f). P, pinacocytes; Cy, cyanobacteria; N, nucleus; S, spicules; C, collagen; and B, bacteria. The scale bars represent 10 μm (a), 5 μm (d) and 1 μm (b, c and e, f).

investigated), which showed more severe disease symptoms. In the Bahamas sponges, flattened pinacocytes were still visible on the surfaces of the orange band transition zone (Fig. 3a). The cyanobacteria were embedded close to the surface within the collagen matrix. TEM revealed large amounts of intracellular cyanobacteria that were apparently subject to digestion by sponge archaeocytes (Fig. 3b and c). By comparison, in the sponges from Florida, pinacocytes were entirely missing on the surface and the cyanobacteria were fully exposed (Fig. 3d). TEM revealed cellular destruction of nearly all cells inspected (Fig. 3e and f).

Chlorophyll *a* analysis

The chlorophyll *a* value of healthy *X. muta* individuals was $32.1 \, \mu g \, g^{-1} \pm 4$ $(n = 9)$ (Fig. 4). The chlorophyll *a* con-
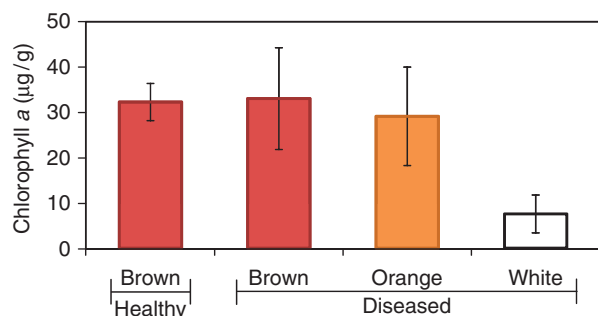
Fig. 4. Chlorophyll *a* concentrations in tissues of healthy ($n = 9 \pm$ SE) and diseased ($n = 3 \pm$ SE) *Xestospongia muta* individuals.

centrations in diseased sponges decreased from brown tissues ($32.9\,\mu\mathrm{g\,g^{-1}} \pm 11.2$, $n = 2$) to orange tissues ($29.9\,\mu\mathrm{g\,g^{-1}} \pm 10$, $n = 3$) to white tissues ($7.5 \pm 4.2\,\mu\mathrm{g\,g^{-1}}$, $n = 3$).

HPLC analysis

HPLC analysis was performed on two healthy and five diseased *X. muta* specimens. Representative chromatograms of one healthy (Fig. 5a) and one diseased sponge are shown (Fig. 5b–d). HPLC analysis of the healthy individual revealed five major peaks (A–E) (Fig. 5a). Five partially pure compounds were identified from these peaks based on UV/MS data and comparison with published *X. muta* metabolites. Peak A represented mutasterol (R_t 6.3 min) (Li *et al.*, 1981), peak B mutafuran A, B, E or F (all of which have equal molecular masses) (R_t 6.9 min) (Morinaka *et al.*, 2007), peak C mutafuran G (R_t 7.0 min) (Morinaka *et al.*, 2007), peak D 18-bromo-octadecadiene-diyonic acid (R_t 7.3 min) (Patil *et al.*, 1992) and peak E 5,28-stigmastadien-3β,24-diol (R_t 7.9 min) (Duque *et al.*, 1985). The HPLC chromatogram of the brown tissue of the diseased sponge showed that the major peaks, including peaks A–E, were still present, albeit at lower concentrations (Fig. 5b). The peak profile was significantly reduced in orange tissues, leaving only a single peak visible (Fig. 5c), and peaks were entirely absent in white tissues of the diseased sponge (Fig. 5d).

DGGE

Inspection of the DGGE gel following amplification with cyanobacteria-specific primers revealed consistently few bands in the healthy sponge and in the brown and orange tissues of the five diseased sponges (Fig. 6a, Table S1). The DGGE banding patterns of the corresponding white tissues were much more heterogeneous. While the conspicuous DGGE bands from the healthy tissues were largely missing, a large number of new bands appeared that formed no consistent pattern. Altogether, 61 bands were excised from the cyanobacterial DGGE gel. Seven bands could not be reamplified with the primers 106f and 781r and were thus
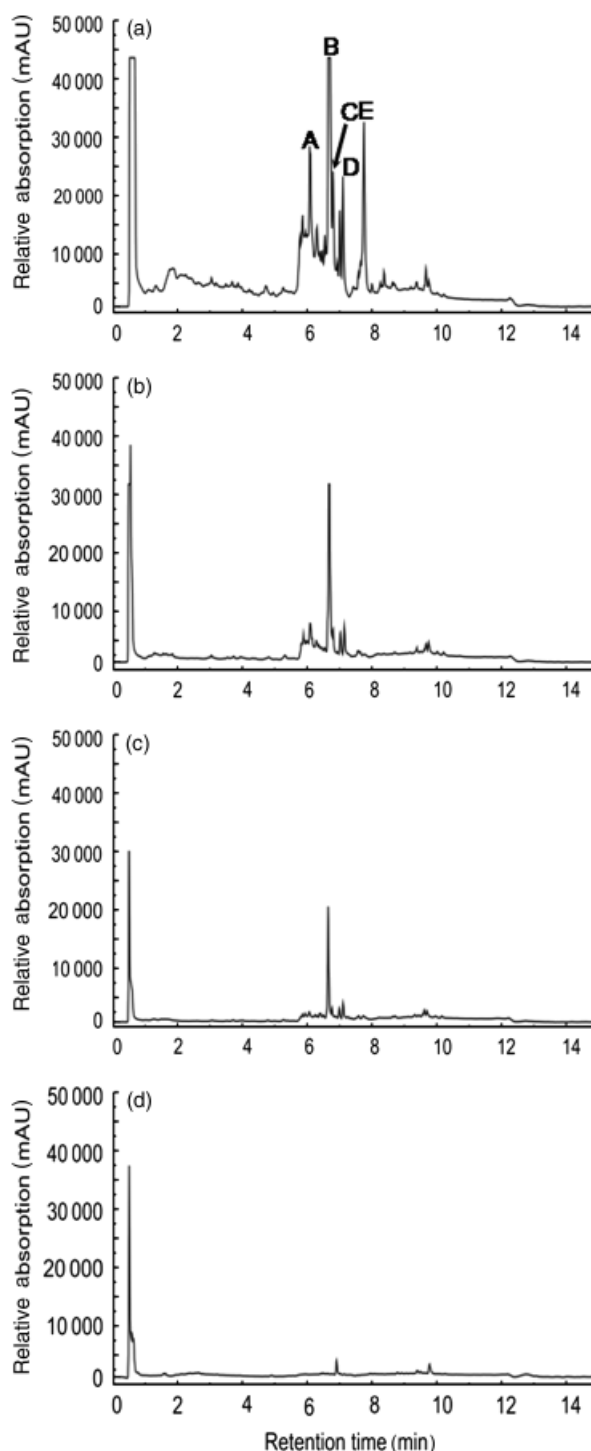

Fig. 5. HPLC chromatograms (at 220 nm) of methanolic extracts obtained from a healthy individual (a) as well as brown (b), orange (c) and white (d) tissues of a diseased *Xestospongia muta* individual (Fig. 1d). The letters A–E depict the identified compounds from the healthy sponge.
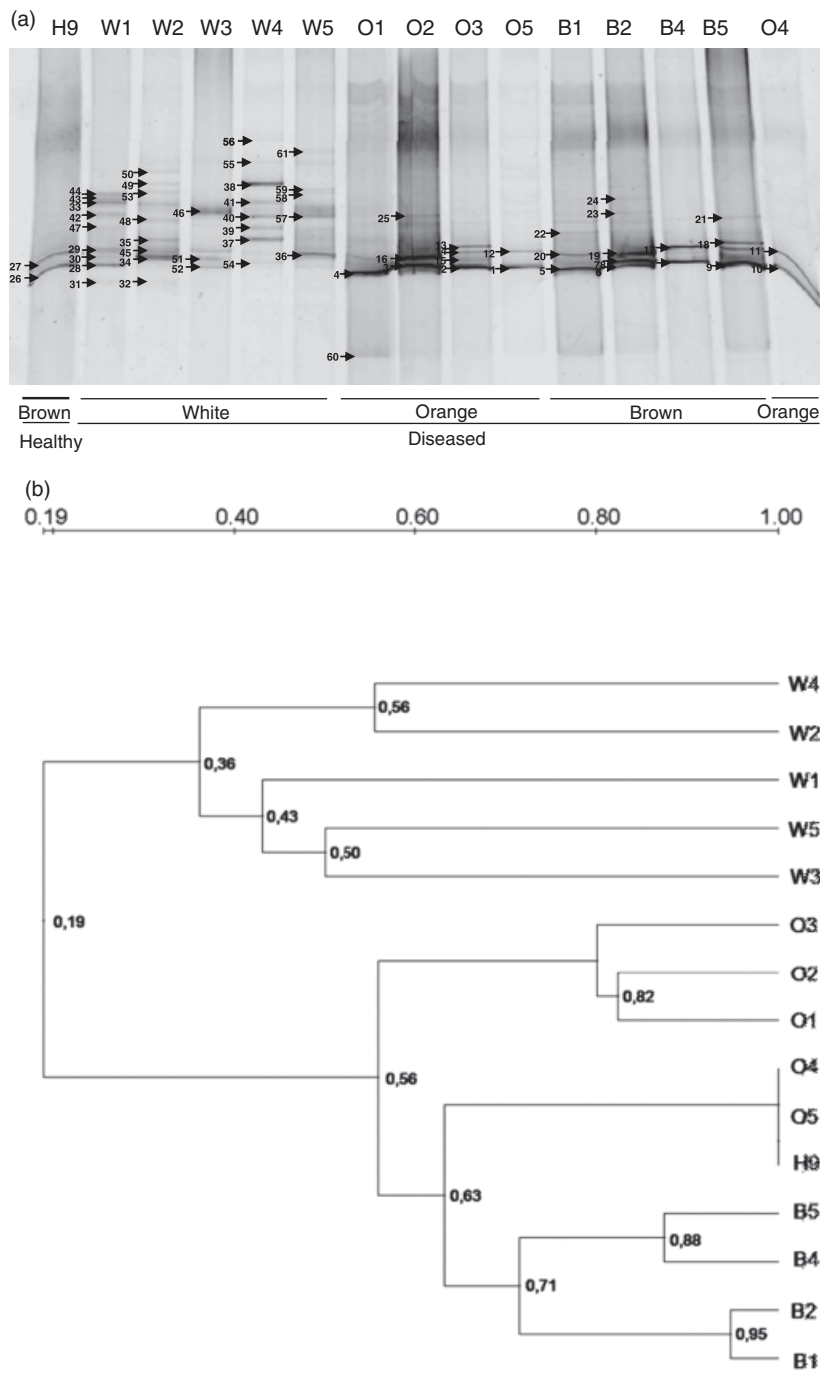
Fig. 6. DGGE of cyanobacterial 16S rRNA genes in one healthy and five diseased *Xestospongia muta* individuals. Arrows point to the excised bands (a). UPGAMA cluster analysis of the cyanobacteria-specific DGGE gel banding pattern (b).

discarded. Up to four clones per DGGE band were sequenced. Four clones belonging to the phylum *Verrucomicrobia* as well as two chimeric sequences were removed from the dataset. Altogether, 58 cyanobacterial 16S rRNA gene sequences were obtained, of which one sequence was derived from healthy *X. muta*, while 17 sequences were derived from brown, 19 sequences from orange and 21 sequences from white tissues of diseased *X. muta* specimens.

The DGGE banding pattern was analyzed using the software program QUANTITY ONE and a dendrogram was constructed using the clustering method UPGAMA (Fig. 6b). The DGGE lanes from white tissues formed one coherent cluster with similarities ranging from 36 to 56%. All DGGE lanes obtained from healthy sponge or from brown and orange tissues of diseased sponges formed another cluster with 56% similarity. Within this, two major groups were

8 DGGE bands, brown: DGGE 8-2, 9, 17-2, 21, orange: DGGE 1, 10, 25-2, 60
X. muta symbiont clone XmA109 (adult), EF159841
X. muta symbiont clone XmE050 (reproductive material), EF159872
DGGE 5, brown
DGGE 16-3, orange
DGGE 34, white
4 DGGE bands, brown: DGGE 18, orange: DGGE 4, 13-3, white: DGGE 61
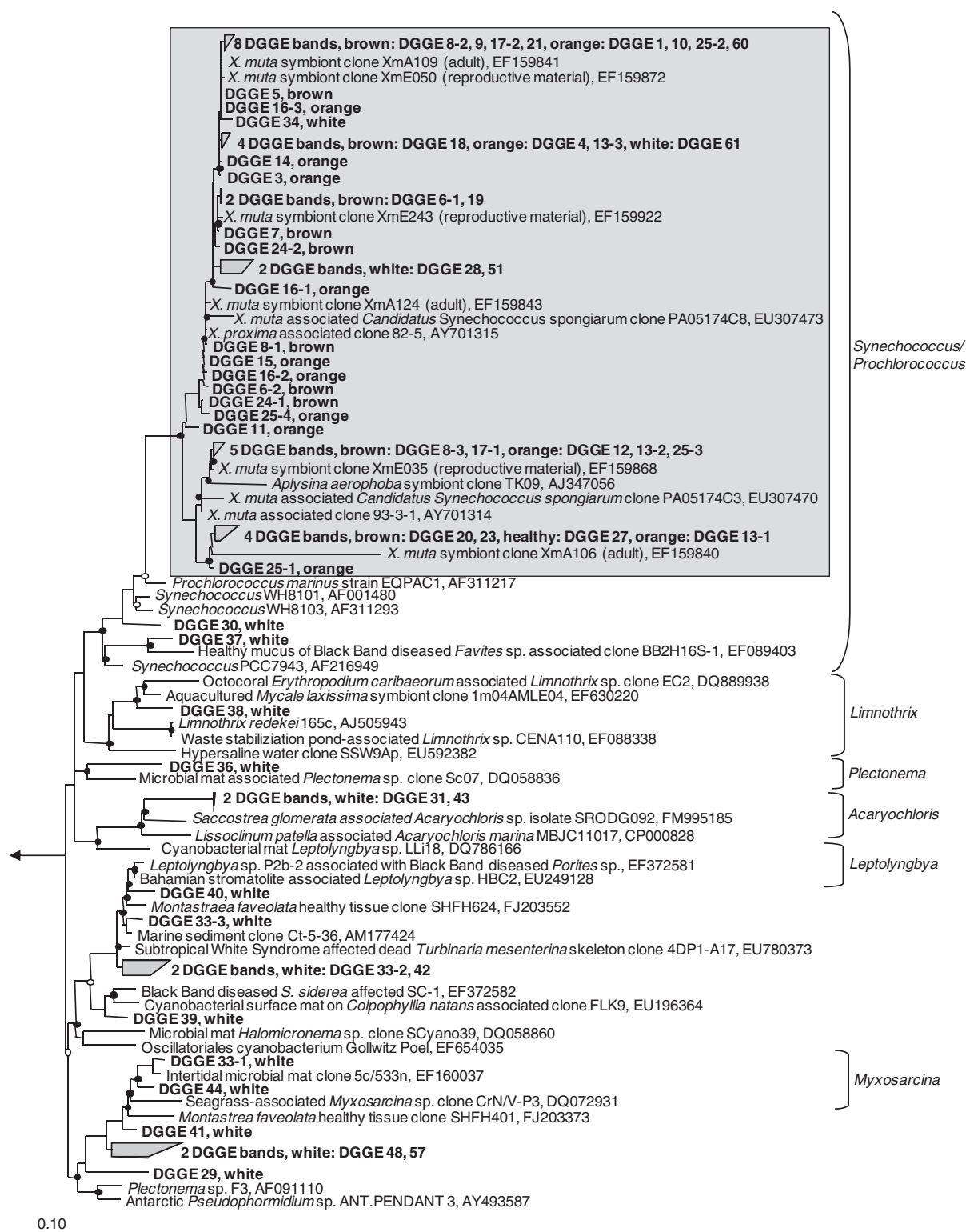DGGE 14, orange
DGGE 3, orange
2 DGGE bands, brown: DGGE 6-1, 19
X. muta symbiont clone XmE243 (reproductive material), EF159922
DGGE 7, brown
DGGE 24-2, brown
2 DGGE bands, white: DGGE 28, 51
DGGE 16-1, orange
X. muta symbiont clone XmA124 (adult), EF159843
X. muta associated *Candidatus* Synechococcus spongiarum clone PA05174C8, EU307473
X. proxima associated clone 82-5, AY701315
DGGE 8-1, brown
DGGE 15, orange
DGGE 16-2, orange
DGGE 6-2, brown
DGGE 24-1, brown
DGGE 25-4, orange
DGGE 11, orange
5 DGGE bands, brown: DGGE 8-3, 17-1, orange: DGGE 12, 13-2, 25-3
X. muta symbiont clone XmE035 (reproductive material), EF159868
Aplysina aerophoba symbiont clone TK09, AJ347056
X. muta associated *Candidatus Synechococcus spongiarum* clone PA05174C3, EU307470
X. muta associated clone 93-3-1, AY701314
4 DGGE bands, brown: DGGE 20, 23, healthy: DGGE 27, orange: DGGE 13-1
X. muta symbiont clone XmA106 (adult), EF159840
DGGE 25-1, orange

Synechococcus/ Prochlorococcus

Prochlorococcus marinus strain EQPAC1, AF311217
Synechococcus WH8101, AF001480
Synechococcus WH8103, AF311293
DGGE 30, white
DGGE 37, white
Healthy mucus of Black Band diseased *Favites* sp. associated clone BB2H16S-1, EF089403
Synechococcus PCC7943, AF216949
Octocoral *Erythropodium caribaeorum* associated *Limnothrix* sp. clone EC2, DQ889938
Aquacultured *Mycale laxissima* symbiont clone 1m04AMLE04, EF630220
DGGE 38, white
Limnothrix redekei 165c, AJ505943
Waste stabiliziation pond-associated *Limnothrix* sp. CENA110, EF088338
Hypersaline water clone SSW9Ap, EU592382
DGGE 36, white
Microbial mat associated *Plectonema* sp. clone Sc07, DQ058836

Limnothrix

Plectonema

2 DGGE bands, white: DGGE 31, 43
Saccostrea glomerata associated *Acaryochloris* sp. isolate SRODG092, FM995185
Lissoclinum patella associated *Acaryochloris marina* MBJC11017, CP000828
Cyanobacterial mat *Leptolyngbya* sp. LLi18, DQ786166
Leptolyngbya sp. P2b-2 associated with Black Band diseased *Porites* sp., EF372581
Bahamian stromatolite associated *Leptolyngbya* sp. HBC2, EU249128
DGGE 40, white
Montastraea faveolata healthy tissue clone SHFH624, FJ203552
DGGE 33-3, white
Marine sediment clone Ct-5-36, AM177424
Subtropical White Syndrome affected dead *Turbinaria mesenterina* skeleton clone 4DP1-A17, EU780373
2 DGGE bands, white: DGGE 33-2, 42
Black Band diseased *S. siderea* affected SC-1, EF372582
Cyanobacterial surface mat on *Colpophyllia natans* associated clone FLK9, EU196364
DGGE 39, white
Microbial mat *Halomicronema* sp. clone SCyano39, DQ058860
Oscillatoriales cyanobacterium Gollwitz Poel, EF654035
DGGE 33-1, white
Intertidal microbial mat clone 5c/533n, EF160037
DGGE 44, white
Seagrass-associated *Myxosarcina* sp. clone CrN/V-P3, DQ072931
Montastrea faveolata healthy tissue clone SHFH401, FJ203373
DGGE 41, white
2 DGGE bands, white: DGGE 48, 57
DGGE 29, white
Plectonema sp. F3, AF091110
Antarctic *Pseudophormidium* sp. ANT.PENDANT 3, AY493587

Acaryochloris

Leptolyngbya

Myxosarcina

0.10

Fig. 7. Phylogenetic maximum likelihood tree with cyanobacterial 16S rRNA gene DGGE sequences and references. Sequences of this study are shown in bold. Full circles indicate bootstrap support ≥ 90% and open circles bootstrap support ≥ 75%. The arrow points towards the outgroup, *Rhodothermus marinus* AF217494. The scale bar indicates 10% sequence divergence. The gray box shows the monophyletic, sponge-specific, cyanobacterial symbiont cluster.
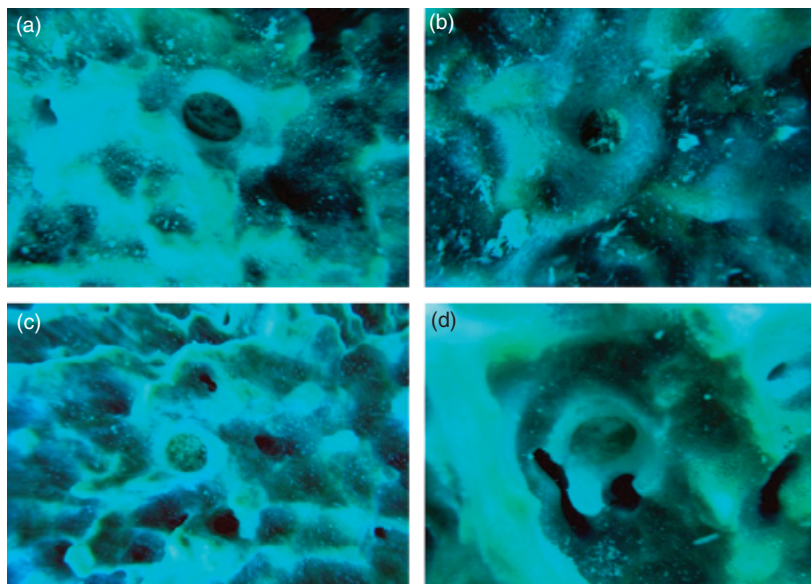
Fig. 8. Underwater photography of the transplanted cores from a healthy individual (a) and from diseased sponges (b–d) into healthy *Xestospongia muta* recipients after 11 days of transplantation.

evident: one comprised of four DGGE lanes from brown tissues (71% similarity) and another one of DGGE lanes from orange tissues (82% similarity). The DGGE lane from the healthy sponge was placed most closely to the DGGE lanes from orange tissues.

Phylogenetic tree construction revealed that all 37 cyanobacterial sequences, which were derived from the healthy sponge as well as from the brown and orange tissues of the diseased sponges, form one coherent, monophyletic sequence cluster together with the previously known *Synechococcus/Prochlorococcus* clade of sponge symbionts (Fig. 7, Table S1). This cluster contains representatives of clades B and L *Synechococcus spongiarum* (Erwin & Thacker, 2008) and also of the vertically transmitted cyanobacterial 16S rRNA gene phylotypes described by Schmitt *et al.* (2008). From the white tissues, only four cyanobacterial DGGE sequences belonged to the cyanobacterial symbiont cluster (DGGE 28, DGGE 34, DGGE 51 and DGGE 61). The remaining 17 sequences from white tissues were affiliated with diverse cyanobacterial genera such as *Limnothrix*, *Plectonema*, *Acaryochloris*, *Leptolyngbya* and *Myxosarcina*. Their closest reference sequences were obtained from freshwater (DGGE 30), seawater (DGGE 57), hypolithic slime (DGGE 43), microbial mat (DGGE 36), rock oyster (DGGE 31), coral reef (DGGE 48) as well as coral sediment (DGGE 29, 33-3, 40), healthy corals (DGGE 33-1, 38, 44, 41), mucus of black band diseased (BBD) corals (DGGE 37) and BBD corals (DGGE 39) as well as from white syndrome affected dead coral skeleton (DGGE 33-2, 42).

Infection experiments

All of the sponges, into which tissue cores had been transplanted, responded in the same manner (Fig. 8). With-

in 11 days the tissues around the cores appeared to heal up. A rejection of the foreign material was not observed. Donor material had been taken from sponges in the early and late stages of disease but no difference in recipient sponge response was observed. Specifically, there was no difference in recipient sponge response to either diseased or healthy cores.

Discussion

Despite the careful characterization of SOB disease of the Caribbean barrel sponge *X. muta*, this study provided no evidence for the involvement of a specific microbial pathogen as an etiologic agent of disease, and attempts at infection with transplanted SOB tissue were not successful. SEM of SOB tissue revealed massive destruction of the pinacoderm accompanied by the loss of both chlorophyll *a* and characteristic secondary metabolites. Electronmicroscopical observations of SOB tissues in the early stage of the disease (Bahamas collection), as judged by the presence of disease symptoms, revealed a notably increased phagocytosis of cyanobacteria that indicates that the host was actively reacting to SOB progression. Tissue from SOB at later stages (Florida collection) exhibited largely degenerated cells. Active phagocytosis of symbiotic cyanobacteria was observed previously in diseased tissues of the mangrove sponge *Geodia papyracea* (Rützler, 1988) and in diseased pustules of *Ircinia* sp. (Maldonado *et al.*, 2010). For cnidarians with algal symbionts, the intriguing hypothesis has been advanced that tissue bleaching is due to an overly aggressive innate immune response, with loss of control over apoptosis and necrosis being the cause of uncontrolled bleaching and ultimately death (Dunn *et al.*, 2004; Weis, 2008). Unraveling the mechanisms of interaction between host phagocytes and

microbial symbionts (i.e. recognition, differentiation between self and nonself) will clearly be instrumental to understanding sponge health and disease.

Microbial community profiling by DGGE revealed a distinct shift from the *Synechococcus/Prochlorococcus* clade of cyanobacterial sponge symbionts in normal sponge tissue towards a heterogeneous mix of cyanobacteria as SOB advances (Figs 6 and 7). Interestingly, several DGGE band sequences of bleached tissues were most closely related to sequences derived from healthy corals (DGGE bands 41, 44), coral mucus (DGGE band 37) or coral disease (DGGE bands 39, 42) (Table S1). The appearance of filament-forming cyanobacterial genera, *Limnothrix*, *Plectonema*, *Leptolyngbya*, in white tissues is consistent with the appearance of filaments in scanning electron microscopy of white *X. muta* tissues (Fig. 2d). Similarly, a shift from a stable bacterial DGGE banding pattern in healthy individuals towards a heterogeneous mixture of DGGE bands in brown, orange and white tissues of SOB sponges was observed (Fig. S2). Moreover, cultivation efforts from the orange band transition zone yielded bacterial isolates most closely related to *Gammaproteobacteria* from BBD-affected corals (data not shown). These data are consistent with previous observations of diseased tissue from the sponge *Aplysina aerophoba* in which shifts from the symbiotic microbiota towards a more diverse microbial consortium were documented (Webster *et al*., 2008b). Several of the pathogenic phylotypes identified in *A. aerophoba* were also most closely related to known BBD coral pathogens. Likewise, bleaching in *X. muta* leads to a disruption of the symbiotic, archaeal ammonia-oxidizing community that was replaced with sediment-derived phylotypes in the late stage of SOB (Lopez-Legentil *et al*., 2010).

Microbial population shifts away from the stable consortium are well known in coral diseases where the change even predates the bleaching event (Cooney *et al*., 2002; Frias-Lopez *et al*., 2002; Pantos *et al*., 2003; Gil-Agudelo *et al*., 2006; Bourne *et al*., 2008). Remarkably, the dominant phylotype during pre- and postbleaching of the coral *Acropora millepora* was a typically sponge-affiliated gammaproteobacterial clade (*Spongiobacter* sp.) (Bourne *et al*., 2008). It thus appears that disturbances of the natural microbiota of sponge and coral hosts are a common feature of disease and that certain opportunistic bacteria are then able to colonize the newly exposed, chemically undefended invertebrate tissues. Whether these bacteria are simply efficient colonizers or whether they actively contribute to the infection process remains to be investigated.

The absence of evidence for a specific pathogen in SOB disease of *X. muta* is noteworthy. Our findings are fully consistent with a recent publication by Luter *et al*. (2010) showing that microorganisms are not responsible for the formation of brown spot lesions in the sponge *Ianthella*

basta. Perhaps most revealing in both studies is the unsuccessful infection of healthy individuals either at early or at late stages of disease (Fig. 8). A previous study also demonstrated that *X. muta* is able to heal wounds very rapidly (Walters & Pawlik, 2005), and this appears to be true whether the wounds are open or filled with exogenous sponge tissue. The infection experiments described in the present study are only the latest attempts at infection by tissue transplantation. Previously, wedges of SOB tissues at various stages of the disease were transplanted into several healthy sponges without inducing SOB in the recipient sponges (data not shown). Consequently, SOB of *X. muta* appears not to be due to the involvement of a microbial pathogen. However, an infectious agent, whether bacterial, fungal or viral, can also not be excluded. Moreover, the earliest window of an infection process may have been missed in this study and methods might be insufficient to identify a pathogen, especially if present at low abundances or if specific factors necessary for the expression of virulence genes were required.

An imbalance of the natural microbial consortia appears to be a hallmark of marine sponge and coral diseases. In this context, it is interesting to note that mostly species belonging to the HMA group of sponges including *X. muta* (Cowart *et al*., 2006), *R. odorabile* (Webster *et al*., 2002), *I. basta* (Cervino *et al*., 2006; Luter *et al*., 2010), *Ircinia* sp. (Maldonado *et al*., 2010), *Aplysina cauliformis* (Olson *et al*., 2006) and *A. aerophoba* (Webster *et al*., 2008b) are prone to disease. As sponge diseases are nearly always reported in the context of environmental stress, the hypothesis put forward by Lesser *et al*. (2007) that coral diseases are, with rare exceptions, opportunistic infections secondary to physiological stress (e.g. elevated seawater temperature) appears to be most plausible also in the context of *X. muta* SOB disease. Indeed, temperature has been identified as a major stress factor in sponges, causing increased heat shock protein gene *hsp70* expression in *X. muta* at temperatures $> 30\,^\circ$C (Lopez-Legentil *et al*., 2008) as well as causing tissue necrosis and dramatic shifts in the microbial community composition of *R. odorabile* $> 33\,^\circ$C (Webster *et al*., 2008a). In conclusion, while microorganisms are clearly instrumental to sponge and coral diseases, we recognize their involvement in maintaining homeostasis in the natural host-associated microbiota rather than in their function as an invading pathogen in the clinical sense.

Acknowledgements

References

Armstrong RA, Singhb H, Torres J *et al.* (2006) Characterizing the deep insular shelf coral reef habitat of the Hind Bank marine conservation district (US Virgin Islands) using the seabed autonomous underwater vehicle. *Cont Shelf Res* **26**: 194–205.

Ashelford KE, Chuzhanova NA, Fry JC, Jones AJ & Weightmann AJ (2005) At least 1 in 20 16S rRNA sequence records currently held in public repositories is estimated to contain substantial anomalies. *Appl Environ Microb* **71**: 7724–7736.

Ashok D, Kokke W, Cochran S, Francis T, Tomszek T & Westley W (1992) Brominated polyacetylenic acids from the marine sponge *Xestospongia muta*: inhibitors of HIV protease. *J Nat Prod* **55**: 1170–1177.

Bourne D, Iida Y, Uthicke S & Smith-Keune C (2008) Changes in coral-associated microbial communities during a bleaching event. *ISME J* **2**: 350–363.

Brusca RC & Brusca GJ (1990) Phylum Porifera: the sponges *Invertebrates*. (Sinauer AD, ed), pp. 181–210. Sinauer Press, Sunderland, MA.

Cerrano C, Bavestrello G, Bianchi CN *et al.* (2000) A catastrophic mass-mortality episode of gorgonians and other organisms in the Ligurian Sea (North-Western Mediterranean), summer 1999. *Ecol Lett* **3**: 284–293.

Cervino JM, Winiarski-Cervino K, Polson SW, Goreau T & Smith GW (2006) Identification of bacteria associated with a disease affecting the marine sponge *Ianthella basta*. New Britain, Papua New Guinea. *Mar Ecol-Prog Ser* **324**: 139–150.

Cooney RP, Pantos O, Le Tissier MD, Barer MR, O'Donnell AG & Bythell JC (2002) Characterization of the bacterial consortium associated with black band disease in coral using molecular microbiological techniques. *Environ Microbiol* **4**: 401–413.

Cowart JD, Henkel TP, McMurray SE & Pawlik JR (2006) Sponge orange band (SOB): a pathogenic-like condition of the giant barrel sponge, *Xestospongia muta*. *Coral Reefs* **25**: 513.

Dunn SR, Thomason JC, Le Tissier MD & Bythell JC (2004) Heat stress induces different forms of cell death in sea anemones and their endosymbiotic algae depending on temperature and duration. *Cell Death Differ* **11**: 1213–1222.

Duque C, Martinez A & Penuela G (1985) Composición esterólica de la esponja marina *Xestospongia muta*. *Rev Colomb Quim* **14**: 81–88.

Erwin PM & Thacker RW (2008) Cryptic diversity of the symbiotic cyanobacterium *Synechococcus spongiarum* among sponge hosts. *Mol Ecol* **17**: 2937–2947.

Frias-Lopez J, Zerkle AL, Bonheyo GT & Fouke BW (2002) Partitioning of bacterial communities between seawater and healthy, black band diseased, and dead coral surfaces. *Appl Environ Microb* **68**: 2214–2228.

Galstoff PS (1942) Wasting disease causing mortality of sponges in the West Indies and Gulf of Mexico. *Proc VIII Amer Sci Cong* **3**: 411–421.

Gammill ER & Fenner D (2005) *Disease Threatens Caribbean Sponges: Report and Identification Guide*. Reefbase. Available at http://www.reefbase.org/spongedisease/

Gil-Agudelo DL, Myers C, Smith GW & Kim K (2006) Changes in the microbial communities associated with *Gorgonia ventalina* during aspergillosis infection. *Dis Aquat Organ* **69**: 89–94.

Harvell CD, Kim K, Burkholder JM *et al.* (1999) Emerging marine diseases-climate links and anthropogenic factors. *Science* **285**: 1505–1510.

Hentschel U, Usher KM & Taylor MW (2006) Marine sponges as microbial fermenters. *FEMS Microbiol Ecol* **55**: 167–177.

Hoegh-Guldberg O, Mumby PJ, Hooten AJ *et al.* (2007) Coral reefs under rapid climate change and ocean acidification. *Science* **318**: 1737–1742.

Hughes TP, Baird AH, Bellwood DR *et al.* (2003) Climate change, human impacts, and the resilience of coral reefs. *Science* **301**: 929–933.

Lesser MP, Bythell JC, Gates RD, Johnstone RW & Hoegh-Guldberg O (2007) Are infectious diseases really killing corals? Alternative interpretations of the experimental and ecological data. *J Exp Mar Biol Ecol* **346**: 36–44.

Li LN, Sjöstrand U & Djerassi C (1981) Minor and trace sterols in marine invertebrates. 19. Isolation, structure elucidation and partial synthesis of 24-methylene-25-ethylcholesterol (mutasterol): first example of sterol side-chain bioalkylation at position 25. *J Am Chem Soc* **103**: 115–119.

Lopez-Legentil S, Song B, Mcmurray SE & Pawlik JR (2008) Bleaching and stress in coral reef ecosystems: hsp70 expression by the giant barrel sponge *Xestospongia muta*. *Mol Ecol* **17**: 1840–1849.

Lopez-Legentil S, Erwin PM, Pawlik JR & Song B (2010) Effects of sponge bleaching on ammonia-oxidizing *Archaea*: distribution and relative expression of ammonia monooxygenase genes associated with the barrel sponge *Xestospongia muta*. *Microb Ecol* **60**: 561–571.

Ludwig W, Strunk O, Westram R *et al.* (2004) ARB: a software environment for sequence data. *Nucleic Acids Res* **32**: 1363–1371.

Luter HM, Whalan S & Webster NS (2010) Exploring the role of microorganisms in the disease-like syndrome affecting the sponge *Ianthella basta*. *Appl Environ Microb* **76**: 5736–5744.

Maldonado M, Sánchez-Tocino L & Navarro C (2010) Recurrent disease outbreaks in corneous demosponges of the genus *Ircinia*: epidemic incidence and defense mechanisms. *Mar Biol* **157**: 1577–1590.

Mao-Jones J, Ritchie KB, Jones LE & Ellner SP (2010) How microbial community composition regulates coral disease development. *PLoS Biol* **8**: e1000345.

McMurray SE, Blum JE & Pawlik JR (2008) Redwood of the reef: growth and age of the giant barrel sponge *Xestospongia muta* in the Florida Keys. *Mar Biol* **155**: 159–171.

McMurray SE, Henkel TP & Pawlik JR (2010) Demographics of increasing populations of the giant barrel sponge *Xestospongia muta* in the Florida Keys. *Ecology* **91**: 560–570.

Morinaka BI, Skepper CK & Molinski TF (2007) Ene-yne tetrahydrofurans from the sponge *Xestospongia muta*. Exploiting a weak CD effect for assignment of configuration. *Org Lett* **9**: 1975–1978.

Muyzer G, Brinkhoff T, Nübel U, Santegoeds C, Schäfer H & Wawer C (1998) Denaturing gradient gel electrophoresis (DGGE) in microbial ecology. *Molecular microbial ecology, manual 3.4.4.* (Akkermans ADL, van Elsas JD & de Bruijn FJ, eds), pp. 1–27. Kluwer Academic Publishers, Dordrecht, the Netherlands.

Nagelkerken I, Aerts L & Pors L (2000) Barrel sponge bows out. *Reef Encounter* **28**: 14–15.

Nübel U, Garcia-Pichel F & Muyzer G (1997) PCR primers to amplify 16S rRNA genes from cyanobacteria. *Appl Environ Microb* **63**: 3327–3332.

Olson JB, Gochfeld DJ & Slattery M (2006) Aplysina red band syndrome: a new threat to Caribbean sponges. *Dis Aquat Organ* **71**: 163–168.

Pantos O, Cooney RP, Le Tissier MD, Barer MR, O'Donnell AG & Bythell JC (2003) The bacterial ecology of a plague-like disease affecting the Caribbean coral *Montastrea annularis*. *Environ Microbiol* **5**: 370–382.

Parsons TR, Maita Y & Lalli C (1984) *A Manual of Chemical and Biological Methods for Seawater Analysis*. Pergamon Press, New York.

Patil AD, Kokke WC, Cochran S, Francis TA, Tomszek T & Westley JW (1992) Brominated polyacetylenic acids from the marine sponge *Xestospongia muta*: inhibitors of HIV protease. *J Nat Prod* **55**: 1170–1177.

Perez T, Garrabou J, Sartoretto S, Harmelin JG, Francour P & Vacelet J (2000) Massive mortality of marine invertebrates: an unprecedented event in northwestern Mediterranean. *CR Acad Sci III* **323**: 853–865.

Perez T, Perrin B, Carteron S, Vacelet J & Boury-Esnault N (2006) *Celtodoryx morbihanensis* gen. nov. sp. nov., a new sponge species (Poecilosclerida, Demospongiae) invading the Gulf of Morbihan (NE Atlantic-France). *Cah Biol Mar* **47**: 205–214.

Pruesse E, Quast C, Knittel K, Fuchs BM, Ludwig W, Peplies J & Glockner FO (2007) SILVA: a comprehensive online resource for quality checked and aligned ribosomal RNA sequence data compatible with ARB. *Nucleic Acids Res* **35**: 7188–7196.

Rosenberg E, Koren O, Reshef L, Efrony R & Zilber-Rosenberg I (2007) The role of microorganisms in coral health, disease and evolution. *Nat Rev Microbiol* **5**: 355–362.

Rützler K (1988) Mangrove sponge disease induced by cyanobacterial symbionts: failure of a primitive immune system? *Dis Aquat Organ* **5**: 143–149.

Sambrook J, Fritsch EF & Maniatis T (1989) *Molecular Cloning: A Laboratory Manual*, 2nd edn. Cold Spring Harbor Laboratory Press, Cold Spring Harbor, NY.

Scheuermayer M, Gulder TA, Bringmann G & Hentschel U (2006) *Rubritalea marina* gen. nov., sp. nov., a marine representative of the phylum 'Verrucomicrobia', isolated from a sponge (Porifera). *Int J Syst Evol Micr* **56**: 2119–2124.

Schmitt S, Angermeier H, Schiller R, Lindquist N & Hentschel U (2008) Molecular microbial diversity survey of sponge reproductive stages and mechanistic insights into vertical transmission of microbial symbionts. *Appl Environ Microb* **74**: 7694–7708.

Steindler L, Huchon D, Avni A & Ilan M (2005) 16S rRNA phylogeny of sponge-associated cyanobacteria. *Appl Environ Microb* **71**: 4127–4131.

Vacelet J & Gallissian M-F (1978) Virus-like particles in cells of the sponge *Verongia cavernicola* (Demospongiae, Dictyoceratida) and accompanying tissue changes. *J Invertebr Pathol* **31**: 246–254.

Vicente VP (1990) Responses of sponges with autotrophic endosymbionts during the coral-bleaching episode in Puerto Rico (West Indies). *Coral Reefs* **8**: 199–202.

Walters KD & Pawlik JR (2005) Is there a trade-off between wound-healing and chemical defenses among Caribbean reef sponges? *Integr Comp Biol* **45**: 352–358.

Webster NS (2007) Sponge disease: a global threat? *Environ Microbiol* **9**: 1363–1375.

Webster NS, Webb RI, Ridd MJ, Hill RT & Negri AP (2001) The effects of copper on the microbial community of a coral reef sponge. *Environ Microbiol* **3**: 19–31.

Webster NS, Negri AP, Webb RI & Hill RT (2002) A spongin-boring α-proteobacterium is the etiological agent of disease in the Great Barrier Reef sponge *Rhopaloeides odorabile*. *Mar Ecol-Prog Ser* **232**: 305–309.

Webster NS, Cobb RE & Negri AP (2008a) Temperature thresholds for bacterial symbiosis with a sponge. *ISME J* **2**: 830–842.

Webster NS, Xavier JR, Freckelton M, Motti CA & Cobb R (2008b) Shifts in microbial and chemical patterns within the marine sponge *Aplysina aerophoba* during a disease outbreak. *Environ Microbiol* **10**: 3366–3376.

Weis VM (2008) Cellular mechanisms of Cnidarian bleaching: stress causes the collapse of symbiosis. *J Exp Biol* **211**: 3059–3066.

Whiteman E (2010) Synopsis: a fatal switch for corals? *PLoS Biol* **8**: e1000346.

Wulff JL (2006) Rapid diversity and abundance decline in a Caribbean coral reef sponge community. *Biol Conserv* **127**: 167–176.

Supporting Information

Additional Supporting Information may be found in the online version of this article:

Fig. S1. Photography on the surface of a healthy *Xestospongia muta* individual (Fig. 1a, #9) and a diseased individual (Fig. 1b).

Fig. S2. DGGE of bacterial 16S rRNA genes in two healthy and five diseased *Xestospongia muta* individuals (a); UPGAMA cluster analysis of the eubacteria-specific DGGE gel banding pattern (b).

Table S1. 16S rRNA gene sequence analysis of the excised cyanobacterial DGGE bands from Fig. 6a.

Please note: Wiley-Blackwell is not responsible for the content or functionality of any supporting materials supplied by the authors. Any queries (other than missing material) should be directed to the corresponding author for the article.